Transmission Line Parameter Estimation Using Traveling-Wave Fault Location Data

Arun Shrestha and Sathish Kumar Mutha,
Schweitzer Engineering Laboratories, Inc.

Presented at the
25th Annual Georgia Tech Fault and Disturbance Analysis Conference
Atlanta, Georgia
May 2–3, 2022

Originally presented at the
75th Annual Conference for Protective Relay Engineers, March 2022

Transmission Line Parameter Estimation Using Traveling-Wave Fault Location Data

Arun Shrestha and Sathish Kumar Mutha, *Schweitzer Engineering Laboratories, Inc.*

Abstract—This paper describes a method to estimate transmission line parameters in traveling-wave (TW) relays. The proposed method uses time-synchronized voltage and current measurements from both ends of a line and TW fault location (TWFL) data available in the event report. Positive-sequence line impedance (Z_1) is estimated using pre-fault positive-sequence quantities. Incremental zero-sequence quantities and TWFL data are used for zero-sequence line impedance (Z_0) estimation. The use of incremental quantities provides better Z_0 estimates for both transposed and untransposed lines. Line parameter estimates from both simulation and field events demonstrate the robustness of the proposed method.

I. Introduction

Transmission line parameters (i.e., positive-sequence and zero-sequence line impedances) are used in power system studies and protective relaying applications, such as power flow calculations, stability analysis, short circuit analysis, relay settings, impedance-based fault location, and relay testing [1]. The positive-sequence impedance (Z_1) can be calculated using the tower configuration and conductor properties. Zero-sequence impedance (Z_0) is usually found to be inaccurate [2], and typically, Z_0 has higher errors than Z_1. Z_0 depends on ground resistivity, which varies with temperature, moisture, mineral content, and compactness [3]. Inaccurate Z_1 and Z_0 impedances can result in overreaching or underreaching issues in distance elements and can lead to misoperation [4]. Similarly, line impedance errors can impact fault location accuracy when impedance-based fault location methods are used.

Reference [2] describes various methods to calculate alternating current (ac) transmission line parameters. These methods use offline and online measurements. Offline methods require the line to be taken out of service and inject signals using test sets. Online methods use synchrophasor data to estimate line parameters. Most of these methods require dedicated equipment, like test sets and phasor measurement units; hence, these methods are costly, labor-intensive, and time-consuming.

This paper describes methods to estimate transmission line parameters using traveling-wave fault location (TWFL) data, time-synchronized voltage, and current measurements from both ends of a line that are available in a traveling-wave (TW) relay event report. Using pre-fault positive-sequence quantities, Z_1 is estimated by solving the PI equivalent line model. A novel incremental zero-sequence quantities-based method is used to estimate Z_0. Incremental zero-sequence quantities are calculated by subtracting zero-sequence quantities from the pre-fault and faulted network. The use of incremental quantities provides better Z_0 estimates for transposed and untransposed lines.

Faults that launch small TWs and certain evolving faults impact the dependability of TW-based and incremental-quantity-based protection elements. For these scenarios, phasor-based protection elements provide backup protection. Phasor-based protection elements require accurate line parameters. The estimated line parameters can be used to check the accuracy of line parameter settings in the relay. When estimated line parameters are used to correct line impedance settings in the TW relay, it increases dependability for phasor-based protection elements. For a non-TW relay (used as backup for a TW relay), the accurate line parameters improve both security and dependability for protection elements and the impedance-based fault locator.

This paper is organized into sections. Section II provides a short summary of various line parameter calculations methods described in the literature. A brief overview of TWFL and incremental quantities is mentioned in Sections III and IV, respectively. Section V describes the proposed line parameter estimation method in detail. Simulation and field results that demonstrate the accuracy of the proposed method are presented in Sections VI and VII. Finally, concluding remarks are presented in Section VIII.

II. Line Parameter Calculation Methods

Line parameter estimation methods can be broadly classified into two groups.

- Offline methods
  - Line constants tools
  - Signal injection methods
  - Event analysis using known fault location
- Online methods
  - Synchrophasor measurements
  - Single-pole open (SPO) method

A. Line Constants Tools

Line constants software tools are widely used in the industry to calculate line parameters. To produce line parameter values, these tools require transmission line data (e.g., tower structure, distance between the phase and ground wires, line sag, ground resistivity, and detailed information of the conductors). Ground resistivity and sag may change based on the ambient conditions, which could cause a variation in the line parameters estimated by these tools. These tools can also model nonhomogenous lines by splitting the transmission line into multiple sections.

B. Signal Injection Methods

Utilities use a signal injection method to determine line parameters from test data. This method requires the line to be taken out of service and inject signals using test sets; hence, this method is expensive and time-consuming. Using field measurements, transmission line equations are solved to calculate line parameters. Field measurements include open-circuit and short-circuit impedance measurements on the line that needs parameters and on adjacent lines that can affect these values. This approach requires safety guidelines and multiple lines to be taken out of service when conducting the tests. Ideally, all the lines that can affect the line parameters should be disconnected during these tests. However, this is not always practical and poses challenges to the accuracy of zero-sequence impedance measurements. In this case, accuracy can be improved by measuring adjacent lines, time-synchronized voltage, and current data. This method is also challenged by ground resistivity and line sag variability. Methods to calculate line parameters for various transmission line configurations are described in detail in [2].

C. Event Analysis Using Known Fault Location

Line parameter settings in protective relays are used to calculate the fault location. If these settings differ from the actual values, the event analysis results in an error of the estimated fault location. However, if we know the accurate fault location from the field and time-synchronized event records from both ends of the line, line parameters can be back-calculated [5]. This method provides accurate estimates for transposed lines and lines without zero-sequence mutual coupling. Untransposed lines and zero-sequence mutual coupling pose as challenges to this method.

D. Synchrophasor Measurements

When synchrophasor measurements are available from both ends of a transmission line, line parameters can be estimated in near real time. A positive-sequence line parameter can be estimated by solving positive-sequence lumped or distributed line models and by using synchrophasor data measured during a normal power system condition [4] [6] [7]. Reference [2] also provides a method to estimate zero-sequence line parameters by using synchrophasor data during breaker SPO conditions. Accurate fault phasors can be obtained with a good amount of fault data; otherwise, it results in estimation errors.

E. SPO Method

This method estimates line parameters using time-synchronized measurements from both terminals of the line when one pole of either terminal is open [4]. A symmetrical component network with one terminal in SPO condition is solved to estimate both positive-sequence and zero-sequence line parameters. This method uses a negative-sequence network to estimate Z_1, because line charging current has a lower effect on the calculation method. This method requires line-side potential transformers (PTs) and an enabled breaker SPO feature. This algorithm can be implemented in line relays capable of exchanging voltage and current signals from the remote terminal.

III. TWFL

Fault location accuracy has improved drastically with the application of TW techniques [8]. Impedance-based fault location methods have also evolved to use remote relay fault information to provide accurate fault location. Single-ended impedance and double-ended impedance methods are two widely used fault location methods in protective relays. Impedance-based fault location methods require Z_1, Z_0, and line length settings. Alternatively, TWFL methods require the line length and TW propagation velocity information. Since TWFL techniques do not use Z_1 and Z_0 settings, errors in impedance line parameters settings have no impact on TWFL.

TWs are step waves that are launched from the fault points and travel away from the fault point, as shown in Fig. 1. The point on the voltage wave other than the zero-voltage point launches these step waves. These waves are transmitted again and are reflected at impedance change points (e.g., line terminals and fault points) [8] [9]. Faults that launch small TWs pose challenges to TWFL. Impedance-based fault location methods and TW-based methods work well together and back up each other.

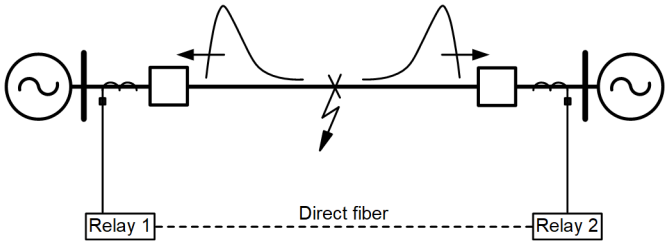

Fig. 1. TWFL in protective relays.

In the single-ended TWFL method, the relay calculates the time difference between the first TW arrival and its reflection from the fault point. This method does not depend on the communication or time-stamped data from the remote relay. However, this method requires processing the reflected wave and poses some challenges using current-based TWs. In the double-ended TWFL (DETWFL) method, the relay calculates the time difference between the TW arrival times at both ends of a transmission line. This method uses the incident waves and not the reflected waves; hence, it simplifies many things in the algorithm implementation. DETWFL requires time-stamped TW information from the remote relay. Equation (1) shows the fault location estimation using the DETWFL method.

$$m = \frac{1}{2}\left[\ell + \left(t_L - t_R\right) \bullet v\right] \tag{1}$$

where:

m = fault location

ℓ = line length setting

t_L = first TW arrival time at the local relay

t_R = first TW arrival time at the remote relay

v = TW propagation velocity

Propagation velocity can be calculated from line energization tests and from external fault event reports. Line energization tests can be conducted by closing one end of the

line breaker while keeping another end breaker open. Based on this test, propagation velocity can be calculated using the line length and time duration between closing of the breaker and the reflected wave. Relay manufacturers recommend using a line energization test to calculate the propagation velocity [9].

DETWFL accuracy depends on the line length setting and propagation velocity setting. DETWFL accuracy also depends on the time-stamping accuracy. Even 1 microsecond of error in time accuracy can cause 300 meters of fault location error. Modern relays have inherent time-stamping accuracy better than 0.2 microseconds, which results in 60 meters of fault location error [8]. Line sag can cause errors in line length estimation, and as a result, affects the propagation velocity estimation. Nevertheless, TWFL methods provide accuracies as low as 300 meters or close to one tower span in real-world fault events [10].

IV. Incremental Quantities

To analyze faults on a transmission line in a complex network, the overall network can be simplified into a two-source power system connected by the transmission line of interest using Thevenin's theorem. Further, the principle of superposition can be used to represent any faulted network as a summation of two separate networks, a pre-fault network, and a pure-fault network. Fig. 2 shows these three networks for a fault on the line with fault resistance, R_F.

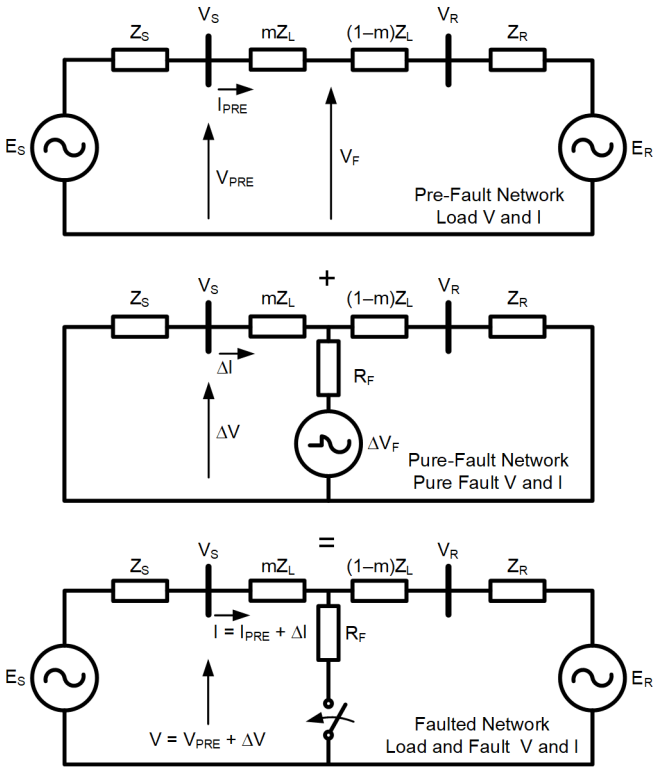

Fig. 2. Faulted network as the superposition of pre-fault network and pure-fault network [11].

The pre-fault network drives the load current through the network and establishes the voltage, V_F, at the fault location. In the pure-fault network, all pre-fault network voltage sources are short-circuited, and the Thevenin source voltage that is equal to the negative pre-fault voltage at the fault location ($-V_F$) is included. The pure-fault network currents and voltages are zero before the fault. Any currents and voltages in the pure-fault network depend only on the network parameters and pre-fault conditions. The pre-fault network provides the initial condition for the pure-fault Thevenin source.

Incremental quantities (i.e., superimposed quantities) represent signals that appear in the pure-fault network [11] [12] [13]. These quantities are typically represented with the delta prefix (Δ) to indicate the change, with respect to the pre-fault network signals. Relays measure both the pre-fault and faulted network signals directly. The incremental voltage and current quantities are expressed in (2).

$$\begin{aligned} \Delta V &= V_{\text{Faulted}} - V_{\text{Pre-fault}} \\ \Delta I &= I_{\text{Faulted}} - I_{\text{Pre-fault}} \end{aligned} \tag{2}$$

The pure-fault network can be solved either in the time-domain or in the frequency domain. In the time-domain, the pure-fault network looks like a lumped parameter resistance, inductance, and capacitance (RLC) network in the transient state. The relationship between incremental voltage and current quantities are governed by differential equations. Protective elements developed by solving incremental quantities in the time-domain have considerable improvement in speed. In the frequency domain, a pure-fault network is solved by using phasors. Algebraic equations govern the relationship between incremental voltage and current quantities. When phasors are used, there is an inherit delay associated with the phasor filter required for accurate phasor estimation. This delay impacts the speed at which phasor-based incremental elements can operate.

In a power network with balanced voltage sources, transposed lines, and balanced loads, only positive-sequence current and voltage exist in the pre-fault network. Negative-sequence and zero-sequence quantities are zero. For such a network, the calculated negative-sequence and zero-sequence quantities in the faulted network are incremental negative-sequence and zero-sequence quantities in the pure-fault network [13]. Positive-sequence incremental quantities are the exception and can be calculated by subtracting positive-sequence quantities between faulted and pre-fault networks.

In practice, transmission lines are often untransposed due to several factors, including the cost [1]. Untransposed lines create unbalance in the pre-fault network and result in the generation of negative-sequence and zero-sequence voltages and currents. These sequence quantities impact performance of many power system components, including protective relaying. With non-zero negative-sequence and zero-sequence quantities in the pre-fault network, incremental negative-sequence and zero-sequence quantities in the pure-fault network are no longer the negative-sequence and zero-sequence quantities in the faulted network. In the next section, we discuss the impact of these quantities in the pre-fault network for line parameter estimation.

VI. Proposed Line Parameter Estimation Method

The proposed method estimates line parameters by postprocessing an event report generated by a TW relay following an internal fault. The event report should contain time-synchronized voltage and current samples from both ends of the transmission line and TWFL data (m_{TW}) for the proposed method to work. The algorithm makes use of pre-fault signals to estimate positive-sequence line impedance (Z_1) and both pre-fault and faulted signals to estimate zero-sequence line impedance (Z_0). TWFL data are only used for estimating zero-sequence line impedance.

For positive-sequence line impedance estimation, positive-sequence network is considered. Line charging current is estimated and subtracted before estimating Z_1. This method is described in Section V Subsection A in detail. Incremental zero-sequence quantities are used to solve zero-sequence pure-fault network for Z_0 estimation. The use of incremental quantities eliminates the impact of pre-fault zero-sequence quantities in zero-sequence impedance calculations. Since a decoupled zero-sequence network is used, this method does not address coupling between sequence networks in a faulted network. Coupling between sequence networks, when unaccounted for, introduces errors in Z_0 estimates. Nevertheless, this method provides better Z_0 estimates for both transposed and untransposed lines, as compared to using the faulted zero-sequence network. Section V Subsection B explains this method in detail.

Fig. 3 shows instantaneous voltage and current samples and phasor magnitudes for an internal Phase-A-to-ground fault. Only Phase A signals from both ends of the lines are shown. Fig. 3 also shows a disturbance detector (DD) binary signal on the fourth subplot. Assertion of the DD is used to identify the fault initiation time (T_{fault_init}). Using the fault initiation time as reference, we can determine the pre-fault data window (PreFltWin) and faulted data window (FltWin). The start time for FltWin depends on the phasor filter used in the relay. The start time is delayed until the phasor filter can estimate faulted phasors accurately. A short time-offset is applied to the PreFltWin to account for delays in the assertion of the DD. The sizes of the PreFltWin and FltWin are determined separately. The phasors in the PreFltWin and FltWin windows are used to calculate pre-fault phasors and faulted phasors for the proposed algorithm. Next, we discuss the proposed estimation method in detail.

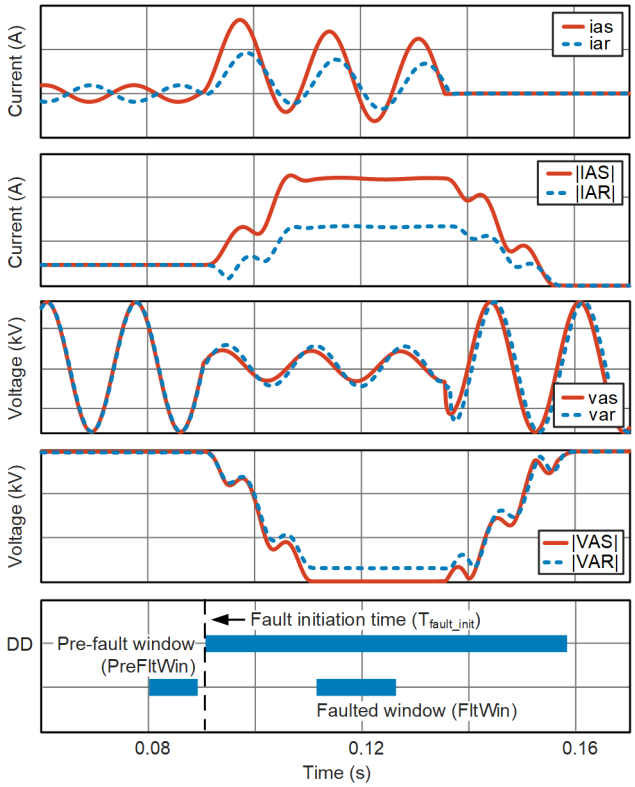

Fig. 3. Event report data showing fault initiation time, pre-fault data window, and faulted data window.

A. Positive-Sequence Line Impedance Estimation

Time-synchronized voltage and current samples from both ends of the transmission lines are available in the event report. We use the PI equivalent model of transmission line and phasors from PreFltWin to estimate the positive-sequence line impedance (Z_1). All calculations are made using phasor data. Estimation of Z_1 using the PI equivalent model and synchronous voltage and current signals are described in [2] and [4].

First, we estimate the positive-sequence (Y_{C1}) and zero-sequence (Y_{C0}) susceptance. Refer to (3).

$$I_{C1} = I_{1S} + I_{1R}$$
$$|X_{C1}| = \frac{|V_{1S} + V_{1R}|}{2 \bullet I_{C1}} \quad (3)$$
$$|Y_{C1}| = \frac{1}{|X_{C1}|}$$

Y_{C0} is assumed 1/1.7 times Y_{C1}. This is based on empirical data. We review a few transmission line parameters (e.g., 33, 132, 220, 400, 765 kilovolts, and single and double circuit towers) and find that the Y_{C1}/Y_{C0} ratio ranges from 1.4 to 1.85. When Y_{C1}/Y_{C0} is set to 3, the errors are slightly higher. Next, we compute self-impedance and mutual-impedance terms [14] and generate a Susceptance Matrix [B]. Refer to (4).

$$B_S = \frac{2 \bullet Y_{C1} + Y_{C0}}{3}$$
$$B_M = \frac{Y_{C0} - Y_{C1}}{3} \quad (4)$$
$$[B] = \begin{bmatrix} B_S & B_M & B_M \\ B_M & B_S & B_M \\ B_M & B_M & B_S \end{bmatrix}$$

By using the Susceptance Matrix [B], the line charging current supplied by the local and remote terminal during pre-fault is calculated. Refer to (5).

$$\begin{bmatrix} I_{AS\_CC'} \\ I_{BS\_CC'} \\ I_{CS\_CC'} \end{bmatrix} = 0.5 \bullet \begin{bmatrix} B_S & B_M & B_M \\ B_M & B_S & B_M \\ B_M & B_M & B_S \end{bmatrix} \bullet \begin{bmatrix} V_{AS} \\ V_{BS} \\ V_{CS} \end{bmatrix}$$
$$\begin{bmatrix} I_{AR\_CC'} \\ I_{BR\_CC'} \\ I_{CR\_CC'} \end{bmatrix} = 0.5 \bullet \begin{bmatrix} B_S & B_M & B_M \\ B_M & B_S & B_M \\ B_M & B_M & B_S \end{bmatrix} \bullet \begin{bmatrix} V_{AR} \\ V_{BR} \\ V_{CR} \end{bmatrix} \quad (5)$$

Next, the line charging current is subtracted from both terminal currents to calculate the current flowing through the line. Refer to (6).

$$\begin{bmatrix} I_{AS'} \\ I_{BS'} \\ I_{CS'} \end{bmatrix} = \begin{bmatrix} I_{AS} \\ I_{BS} \\ I_{CS} \end{bmatrix} - \begin{bmatrix} I_{AS\_CC'} \\ I_{BS\_CC'} \\ I_{CS\_CC'} \end{bmatrix}$$
$$\begin{bmatrix} I_{AR'} \\ I_{BR'} \\ I_{CR'} \end{bmatrix} = \begin{bmatrix} I_{AR} \\ I_{BR} \\ I_{CR} \end{bmatrix} - \begin{bmatrix} I_{AR\_CC'} \\ I_{BR\_CC'} \\ I_{CR\_CC'} \end{bmatrix} \quad (6)$$

Once the line charging current is subtracted, the positive-sequence current ($I_{1S'\_Pre\text{-}fault}$) through the line is calculated. By using the positive-sequence voltage and current phasors, the positive-sequence impedance (Z_1) is estimated for the PreFltWin data window. Refer to (7).

$$Z_1 = \frac{V_{1S\_Pre\text{-}fault} - V_{1R\_Pre\text{-}fault}}{I_{1S'\_Pre\text{-}fault}} \quad (7)$$

Finally, we discard the maximum and minimum value estimated for the PreFltWin data window and average the rest for a positive-sequence line impedance (Z_1) estimate. Similarly, the average zero-sequence voltage and currents ($V_{0S\_Pre\text{-}fault}$, $I_{0S'\_Pre\text{-}fault}$, $V_{0R\_Pre\text{-}fault}$, $I_{0R'\_Pre\text{-}fault}$) are also calculated using PreFltWin data. These pre-fault sequence quantities and the calculated Susceptance Matrix [B] are used for zero-sequence line impedance estimation, as discussed in the next subsection.

B. Zero-Sequence Line Impedance Estimation

The zero-sequence line impedance is only estimated if the fault type is identified as a line-to-ground fault (LG) or double line-to-ground fault (LLG) in the event report. For faults involving ground, convert the TWFL data in the event report to a per-unit value (m_{TW}). Refer to (8).

$$m_{TW} = \frac{\text{Traveling-Wave Fault Location Data}}{\text{Line Length (LL)}} \quad (8)$$

Using the Susceptance Matrix [B] calculated earlier, the line charging current for the FltWin data window is calculated, as shown in (9). All calculations are made using phasors.

$$\begin{bmatrix} I_{AS\_CC''} \\ I_{BS\_CC''} \\ I_{CS\_CC''} \end{bmatrix} = m_{TW} \bullet \begin{bmatrix} B_S & B_M & B_M \\ B_M & B_S & B_M \\ B_M & B_M & B_S \end{bmatrix} \bullet \begin{bmatrix} V_{AS} \\ V_{BS} \\ V_{CS} \end{bmatrix}$$
$$\begin{bmatrix} I_{AR\_CC''} \\ I_{BR\_CC''} \\ I_{CR\_CC''} \end{bmatrix} = (1 - m_{TW}) \bullet \begin{bmatrix} B_S & B_M & B_M \\ B_M & B_S & B_M \\ B_M & B_M & B_S \end{bmatrix} \bullet \begin{bmatrix} V_{AR} \\ V_{BR} \\ V_{CR} \end{bmatrix} \quad (9)$$

Next, the line charging current in the faulted network is subtracted from both terminal currents. Refer to (10).

$$\begin{bmatrix} I_{AS''} \\ I_{BS''} \\ I_{CS''} \end{bmatrix} = \begin{bmatrix} I_{AS} \\ I_{BS} \\ I_{CS} \end{bmatrix} - \begin{bmatrix} I_{AS\_CC''} \\ I_{BS\_CC''} \\ I_{CS\_CC''} \end{bmatrix}$$
$$\begin{bmatrix} I_{AR''} \\ I_{BR''} \\ I_{CR''} \end{bmatrix} = \begin{bmatrix} I_{AR} \\ I_{BR} \\ I_{CR} \end{bmatrix} - \begin{bmatrix} I_{AR\_CC''} \\ I_{BR\_CC''} \\ I_{CR\_CC''} \end{bmatrix} \quad (10)$$

Once the line charging current is subtracted, zero-sequence voltage and current quantities ($V_{0S\_Faulted}$, $I_{0S''\_Faulted}$, $V_{0R\_Faulted}$, $I_{0R''\_Faulted}$) in the faulted network are calculated for both ends of the line. Next, zero-sequence quantities of the pre-fault network are subtracted from the faulted network to calculate incremental zero-sequence quantities. These incremental zero-sequence phasors are generated by the pure-fault network. Refer to (11).

$$\Delta V_{0S} = V_{0S\_Faulted} - V_{0S\_Pre\text{-}fault}$$
$$\Delta I_{0S''} = I_{0S''\_Faulted} - I_{0S'\_Pre\text{-}fault}$$
$$\Delta V_{0R} = V_{0R\_Faulted} - V_{0R\_Pre\text{-}fault}$$
$$\Delta I_{0R''} = I_{0R''\_Faulted} - I_{0R'\_Pre\text{-}fault} \quad (11)$$

Fig. 4 shows the equivalent zero-sequence network for a pure-fault network. The pure-fault network includes incremental zero-sequence voltage and current phasor quantities.

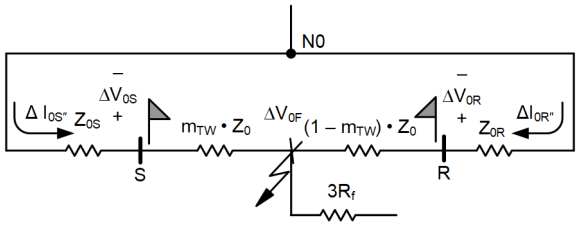

Fig. 4. Equivalent zero-sequence network for pure-fault network.

By using incremental zero-sequence phasors in the pure-fault network, zero-sequence line impedances (Z_0) are estimated for FltWin data window. Maximum and minimum calculated values are discarded, and an average of the remaining estimates is the Z_0 estimate for the given line. Refer to (12).

$$Z_0 = \frac{\Delta V_{0S} - \Delta V_{0R}}{m_{TW} \bullet \Delta I_{0S''} - (1 - m_{TW}) \bullet \Delta I_{0R''}} \quad (12)$$

For a network with unbalanced loads and untransposed transmission lines, the pre-fault negative-sequence and zero-sequence quantities are not zero. This unbalance creates small negative-sequence and zero-sequence quantities in the pre-fault network. When the faulted network zero-sequence quantities are used to estimate zero-sequence line impedance, it results in significant errors. Using pure-fault incremental zero-sequence quantities improves Z_0 estimates. In Section VI, we present test results that show improvement in line parameter estimation when incremental zero-sequence quantities are used.

C. Phenomena That Impact Estimation Accuracy

The proposed method estimates Z_1 using positive-sequence voltages from both ends of the line and the positive-sequence current flowing through the line. Inaccuracies in current transformers (CTs), PTs, and relay measurement circuits result in voltage and current measurements errors in the relay. An inaccurate measurement leads to errors in line parameter estimation. For a small load angle delta between two ends of the line, small CT and PT errors are greatly amplified [4]. As a result, Z_1 estimates have high errors for a load angle delta less than 5 degrees. For long transmission lines, the PI equivalent model cannot accurately represent line charging current. This leads to an error in through currents and impacts Z_1 estimates.

Incremental zero-sequence quantities and TWFL data are used to estimate Z_0 in the proposed method. Faults occurring at voltage zero do not launch any TWs. Any phenomenon that impacts TW and any inaccuracies in TWFL have direct impact on the accuracy of Z_0 estimates. The impact of TWFL inaccuracy on Z_0 estimates is demonstrated with simulation results in Section VI. Incremental zero-sequence quantities are calculated by using zero-sequence quantities from the pre-fault and faulted network. Evolving faults, CT saturation, coupling capacitor voltage transformers (CCVT) transients, faults with time-varying fault resistance, and fast breaker operation impact the accuracy of zero-sequence quantities estimated by the relay. Errors in incremental zero-sequence quantities impact the accuracy of Z_0 estimates. The proposed method does not incorporate the effect of zero-sequence mutual impedance for Z_0 estimates. If mutually coupled lines are present, it adversely affects the accuracy of Z_0 estimation.

With untransposed lines, sequence networks are no longer independent. Positive-sequence current flowing in an unbalanced system produces voltage drops in all three sequence networks [15]. Similarly, negative-sequence and zero-sequence current also produces voltage drops in all three sequence networks. The proposed method only subtracts the zero-sequence quantities from the pre-fault network. However, it does not account for the coupling of positive-sequence and negative-sequence quantities on the pure-fault zero-sequence network. The coupling of sequence networks affects Z_0 estimation accuracy.

Like the proposed Z_0 estimation method, Z_1 can be estimated using pure-fault negative-sequence incremental quantities. The coupling of the two remaining sequence networks on the negative-sequence network is relatively stronger compared to the zero-sequence network. As the coupling of sequence networks is not accounted in the calculation, Z_1 estimates using pure-fault negative-sequence incremental quantities have higher errors than the estimates provided by the proposed method. The proposed methods for Z_1 and Z_0 estimates provide better results than simply using the sequence quantities from the faulted network.

VII. Simulation Results

This section provides test results from real-time simulation and provides results for the proposed estimation method. We model the two-source power system (shown in Fig. 5) in a real-time digital simulator. Line and source parameters are provided in the Appendix. The system nominal voltage is 400 kilovolts, and the line length is 100 kilometers.

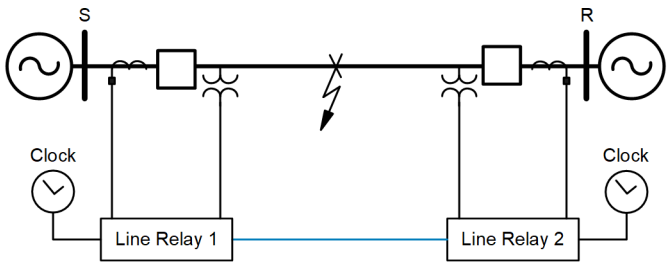

Fig. 5. Test setup used for real-time simulation.

The power system is modeled along with CT, CCVT, and two-cycle circuit breakers [16]. Two TW line relays are connected to the CT and CCVT outputs and configured to protect the 400 kilovolts line. For any internal fault, both line relays issue trip signals to isolate the fault. Event reports are triggered for every internal fault, and each event report contains time-synchronized voltage and current signals from both terminals of the line. The event report also contains other important information like fault type and DD binary signal. Event reports generated by Line Relay 1 at Terminal S are used for line parameter estimation. Because of the limitations of the simulation hardware, TWFL is not tested with the setup. The fault location is assumed to be known when executing the line parameter estimation algorithm. Later, we show the impact of TWFL variation on the estimates.

For a given test scenario, a total of 81 fault cases are simulated using the combination of load angle, fault type, fault resistance, and fault location, as shown in the following bullets.

- Load angle (δ): 20°, 1°, –20°
- Fault resistance (R_f): 0, 10, 40 ohms
- Fault type: AG, BC, CAG
- Fault location (m_{TW}): 30, 50, 80 kilometers

A. Transposed Line Model—Faulted Network Method

In the first test scenario, the transmission line is modeled as a transposed line. As expected, the pre-fault negative-sequence and zero-sequence quantities are zero. With zero pre-fault negative-sequence and zero-sequence quantities, the incremental quantities are equal to negative-sequence and zero-sequence quantities in the faulted network. Assuming the fault

location is known, Z_1 and Z_0 are estimated using Equations (13) and (14) by solving the faulted negative-sequence and zero-sequence network. Fig. 6 and Fig. 7 show the estimated Z_1 and Z_0 for 81 fault cases, as described previously. In both figures, the triangle, circle, and diamond represent line parameter estimates for faults at 30, 50, and 80 kilometers, respectively. With this method, the inaccuracy of estimated values for faults at 30 kilometers is slightly higher that 5 percent.

$$Z_1 = \frac{V_{2S} - V_{2R}}{m_{TW} \bullet I_{2S} - (1 - m_{TW}) \bullet I_{2R}} \quad (13)$$

$$Z_0 = \frac{V_{0S} - V_{0R}}{m_{TW} \bullet I_{0S} - (1 - m_{TW}) \bullet I_{0R}} \quad (14)$$

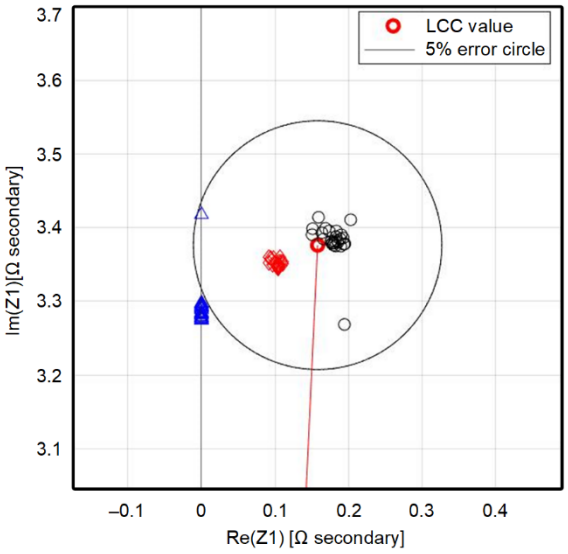

Fig. 6. Z_1 estimates for a transposed line model using the faulted network method.

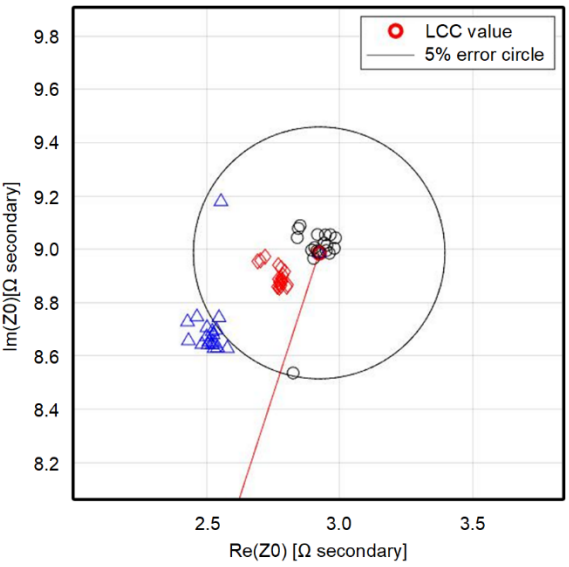

Fig. 7. Z_0 estimates for a transposed line model using the faulted network method.

B. *Untransposed Line Model—Faulted Network Method*

For the second test scenario, the transmission line was modeled as an untransposed line. In reality, most transmission lines are often untransposed due to several factors, including the cost [2]. Untransposed lines lead to unbalance in three phases and result in the generation of negative-sequence and zero-sequence voltages and currents. With untransposed lines, sequence networks are no longer independent. Positive-sequence current flowing in an unbalanced system produces voltage drops in all three sequence networks [15]. Similarly, negative-sequence and zero-sequence current also produces voltage drops in all three sequence networks. If a sequence network is used by ignoring the voltage drops created by two remaining sequence networks, it impacts accuracy.

Assuming the fault location is known, Z_1 and Z_0 are estimated using Equations (13) and (14) by using the faulted data window. Fig. 8 and Fig. 9 show the estimated values Z_1 and Z_0. The inaccuracy of estimated values is high. These two figures demonstrate that we cannot use Equations (13) and (14) to estimate line parameters for untransposed lines.

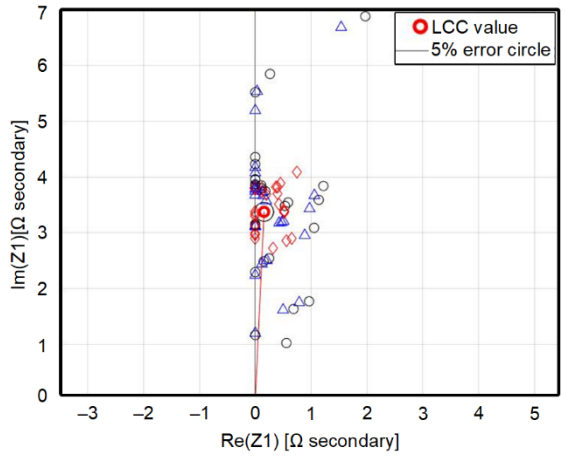

Fig. 8. Z_1 estimates for an untransposed line model using the faulted network method.

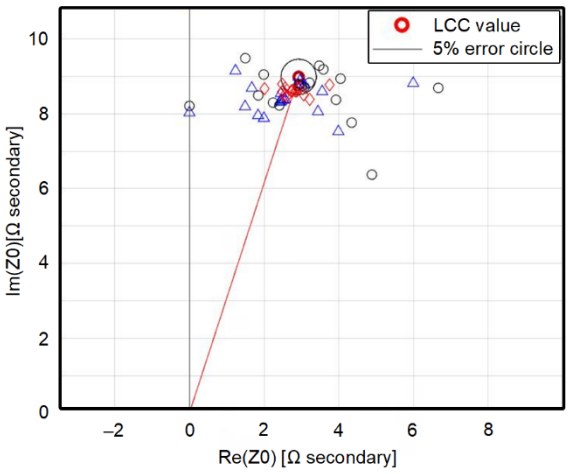

Fig. 9. Z_0 estimates for an untransposed line model using the faulted network method.

C. *Untransposed Line Model—Proposed Method*

In this test scenario, the transmission line is modeled as an untransposed line and line parameters are estimated using the proposed method described in Section VI. Again, we assume that accurate fault location for each of the 81 faults is known. Z_1 and Z_0 estimates for this test scenario are shown in Fig. 10 and Fig. 11, respectively. The estimated line parameters are within 5-percent of the error threshold. Z_1 estimates depend on the pre-fault positive-sequence voltage and current, and they are not impacted by fault locations. As indicated by the cluster of Z_0 estimates for a given fault location in Fig. 11, the accuracy of the zero-sequence line parameter estimation depends on the fault location. In both figures, the triangle, circle, and diamond represent line parameter estimates for faults at 30, 50, and 80 kilometers, respectively.

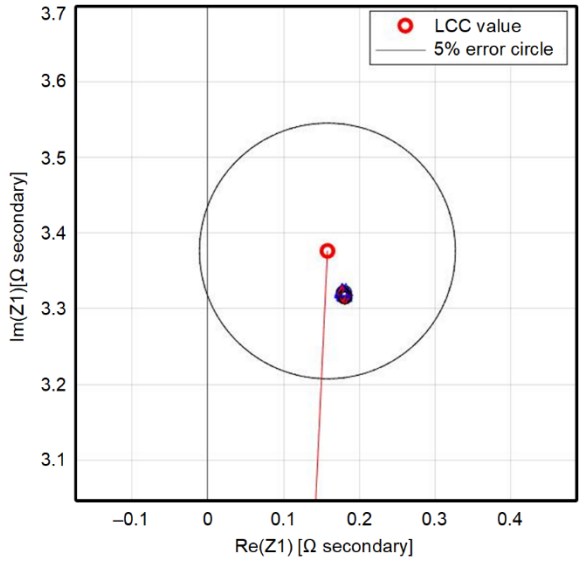

Fig. 10. Z_1 estimates for an untransposed line model using the proposed method.

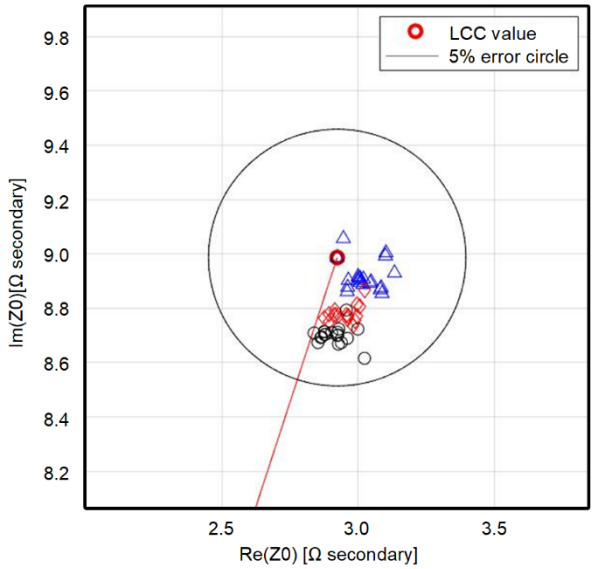

Fig. 11. Z_0 estimates for an untransposed line model using the proposed method.

D. *Untransposed Line Model—TWFL Inaccuracy of ±300 Meters*

In this test scenario, we study the impact of TWFL inaccuracy on the proposed line parameter estimation method. As discussed earlier, Z_1 estimates have no dependence on the TWFL data. It only impacts Z_0 estimates.

The double-ended TW-based fault-locating method is very accurate and has a field-proven track record [8]. When the TW-based line relay is configured correctly, the field reports fault location errors that are within one tower span (300 meters) on average. Using the event reports from the previous subsection, Z_0 are re-estimated by adding TWFL error of +300 meters. Fig. 12 shows Z_0 estimates for this scenario. Z_0 estimates for the faults at 30 kilometers (triangles) are affected the most by TWFL inaccuracy of +300 meters, followed by the faults at 50 kilometers (circles) and the faults at 80 kilometers (diamond). This proves that Z_0 estimates is affected by inaccuracy of TWFL as a percentage of the actual fault location. For the same TWFL inaccuracy of +300 meters, the Z_0 estimated error is higher for faults close to the relay terminal.

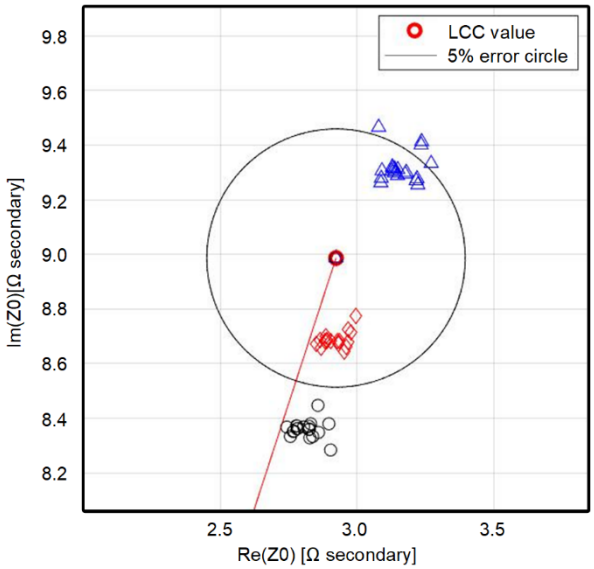

Fig. 12. Z_0 estimates for an untransposed line model using the proposed method with +300 meters TWFL inaccuracy.

Next, Z_0 line parameters are re-estimated using the proposed method and by adding TWFL inaccuracy of –300 meters. Fig. 13 shows the Z_0 estimates for all 81 faults. The TWFL inaccuracy has the most impact on the faults at 30 kilometers. As compared to the previous case, the Z_0 estimates for faults at 30 kilometers are smaller than the actual transmission line Z_0 value.

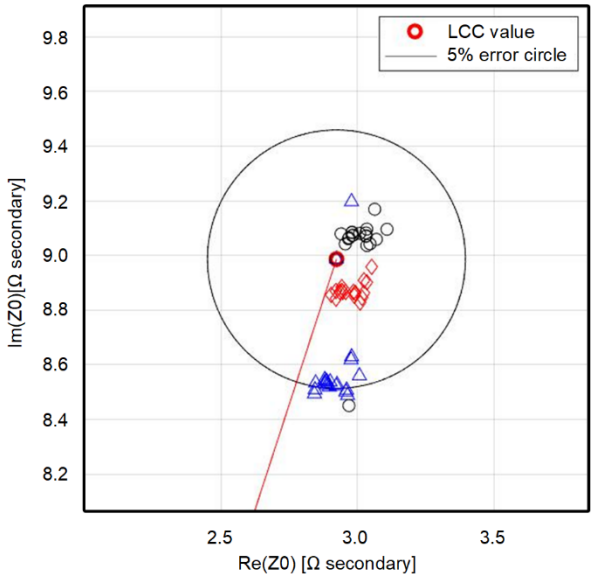

Fig. 13. Z_0 estimates for an untransposed line model using the proposed method with –300 meters TWFL inaccuracy.

Fig. 14 shows the impact of TWFL inaccuracy on Z_0 estimates for a fault at 30 kilometers. The TWFL error has minimum impact on the Z_0 phase angle. However, Z_0 magnitude error increases linearly with an error in TWFL data.

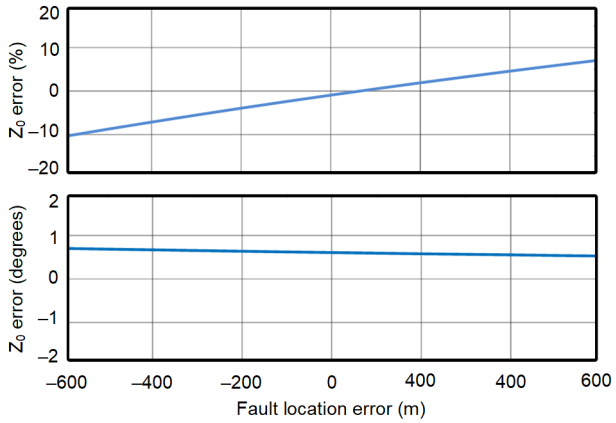

Fig. 14. Z_0 magnitude and phase angle error due to inaccuracy in TWFL.

VIII. Field Results

Following the simulation results, we estimate line parameters using event reports from TW relays for real-world faults. We analyze five event reports from four different transmission lines. Events 2A and 2B are for two different faults on the same transmission line. For each event, line parameters are estimated using the proposed method and the TWFL data stored in the event report. Relay line parameter settings, estimated Z_1/Z_0 values, and errors (with respect to the relay settings for each field event) is tabulated in Table I. The results tabulated in Table I are generated by using event reports from the local relays. Line parameters are also estimated using event reports and TWFL data from the remote relays. The results are similar for both cases.

Fig. 15 shows the voltage and current signals from both line terminals for an internal CG fault for Event 1. The relays at both terminals detect and isolate the fault by opening Breaker Pole C. The TW relay estimates the fault location at 60.995 miles from the local terminal. The fault location of 61.501 miles is confirmed by the field. Fig. 16 shows the sequence quantities and binary signals required to run the proposed line parameter estimates. The proposed method estimates Z_1 as 22.86 ∠80.75° ohms secondary and Z_0 as 48.81 ∠73.78° ohms secondary, respectively. When compared with line impedance magnitude settings in the relay, the errors are 2.82 percent for Z_1 and 4.75 percent for Z_0.

Except for Events 2A and 2B, the estimated Z_1 values are within 5-percent magnitude error and 1-degree phase angle error of the relay settings. For these two events, the load angles δ (∠V1S – ∠V1R) in PreFltWin are 1 degree and 1.4 degrees, respectively. When PI equivalent model of transmission line is used, Z_1 estimates have high error for load angle less than 5 degrees [4]. For small load angle, small CT and VT errors are greatly amplified, leading to inaccurate Z_1 estimates.

Event 3 has the highest magnitude and phase angle error for Z_0 estimates. The error can be the result of various power system phenomena, as described in Section VI. Event 4 is an AB fault, and as a result, only Z_1 is estimated for this event.

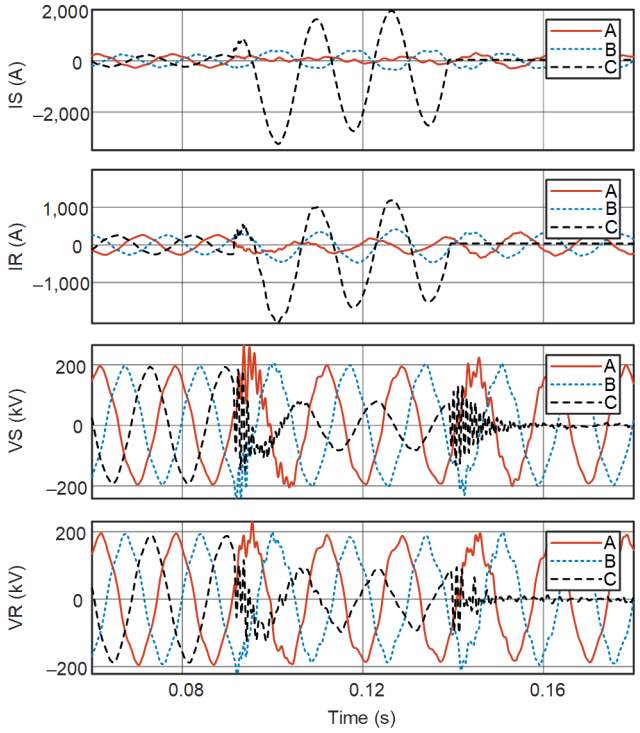

Fig. 15. Voltage and current signals from both line terminals for Event 1.

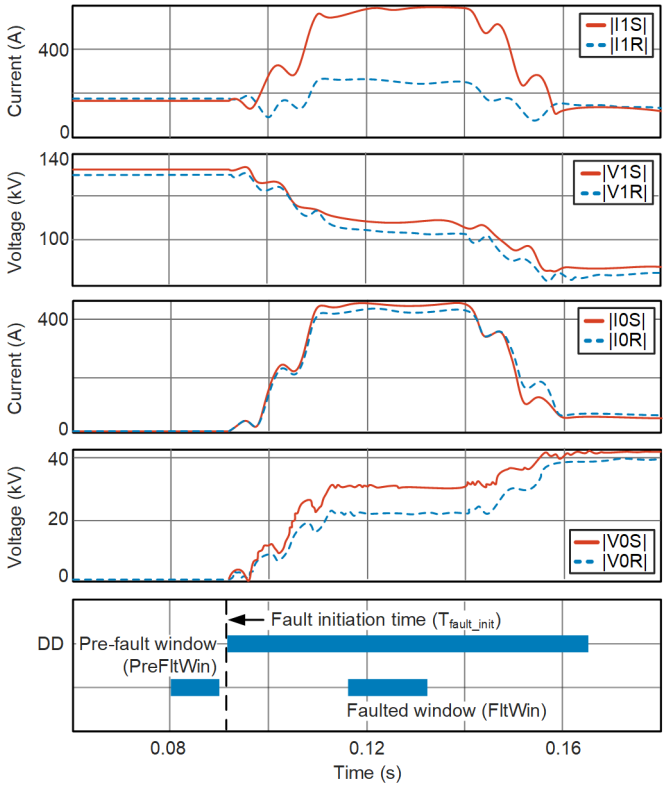

Fig. 16. Local relay event report data for Event 1.

IX. Conclusion

Inaccurate Z_1 and Z_0 impedances can result in overreaching or underreaching issues in distance element applications and can lead to misoperation. Similarly, errors in line impedance can impact fault location accuracy when impedance-based fault location methods are used. Line parameters estimation using signal injection methods are costly, labor-intensive, and time-consuming.

This paper presents a method to estimate transmission line parameters using TWFL data and time-synchronized voltage and current measurements from both ends of a line available in TW relay's event reports. The line parameter estimates include CT and VT errors. A novel incremental zero-sequence quantities-based method is used to estimate Z_0, which provides better Z_0 estimates for both transposed and untransposed lines. The accuracy of line parameter estimates provided by the proposed method is demonstrated by using simulation and field events.

This method requires an event report with time-synchronized voltage and current samples from both ends of the transmission line. A small load angle impacts the accuracy of Z_1 estimates. Evolving faults, CT saturation, CCVT transients, faults with time-varying fault resistance, and fast breaker operation impact accuracy of Z_0 estimates. The accuracy of TWFL directly impacts Z_0 estimates. The proposed method does not incorporate the effect of zero-sequence mutual impedance for Z_0 estimates. If mutually coupled lines are present, it adversely affects the accuracy of Z_0 estimation.

X. Appendix

The parameters for the 400 kilovolts overhead transmission line are listed in Table I and Table II.

Table I
Line Parameter Estimation Using Field Event Reports

Event #	Line voltage (kV)	Fault type	Fault location (miles)		Relay settings	Z_1/Z_0 estimates	[Mag error, phase error]
			Actual	DETWFL			
1	230	CG	61.501 (Local), 91.669 (Remote)	60.995 (Local), 92.175 (Remote)	$Z_1 = 23.53\angle 81.71°$ $Z_0 = 46.6\angle 81.14°$	$Z_1 = 22.86\angle 80.75°$ $Z_0 = 48.81\angle 73.78°$	Z_1 = [2.82%, 0.96°] Z_0 = [4.75%, 7.35°]
2A	220	BG	33.867 (Local), 28.085 (Remote)	33.837 (Local), 28.143 (Remote)	$Z_1 = 5.22\angle 79.54°$ $Z_0 = 12.72\angle 75.74°$	$Z_1 = 5.70\angle 76.94°$ $Z_0 = 12.32\angle 72.68°$	Z_1 = [9.19%, 2.59°] Z_0 = [3.08%, 3.05°]
2B	220	BG	33.867 (Local), 28.085 (Remote)	33.908 (Local), 28.072 (Remote)	$Z_1 = 5.22\angle 79.54°$ $Z_0 = 12.72\angle 75.74°$	$Z_1 = 5.63\angle 80.09°$ $Z_0 = 11.92\angle 73.17°$	Z_1 = [7.99%, 0.55°] Z_0 = [6.29%, 2.57°]
3	115	AG	3.1(Local), 54.66 (Remote)	3.199 (Local), 54.504 (Remote)	$Z_1 = 5.91\angle 69.21°$ $Z_0 = 18.97\angle 69.2°$	$Z_1 = 6.1488\angle 70.25°$ $Z_0 = 17.52\angle 78.48°$	Z_1 = [4.04%, 1.04°] Z_0 = [7.63%, 9.28°]
4	132	AB	32.593 (Local), 26.443 (Remote)	32.665 (Local), 26.375 (Remote)	$Z_1 = 2.61\angle 64°$ $Z_0 = 7.24\angle 66.66°$	$Z_1 = 2.72\angle 63.11°$	Z_1 = [4.24%, 0.88°]

TABLE II
LINE PARAMETERS FOR A 400 KILOVOLT OVERHEAD LINE

Line parameters	**Values**
Phase conductor outside diameter	3.177 cm
Phase conductor thickness/diameter ratio (T/D)	0.5
Phase conductor dc resistance	0.0547 Ω/km
Number of bundled conductors per phase	4
Shield conductor outside diameter	0.824 cm
Shield conductor thickness/diameter ratio (T/D)	0.5
Shield conductor dc resistance	0.8525 Ω/km
Number of bundled conductors per shield	1
Horizontal tower configuration (A – B – C – Shield1 – Shield2)	(0 – 11 – 22 – 2.97 – 19.03) m
Vertical tower configuration (A – B – C – Shield1 – Shield2)	(21.798 – 21.798 – 21.798 – 29.27 – 29.27) m
Vertical mid-span configuration (A – B – C – Shield1 – Shield2)	(8.84 – 8.84 – 8.84 – 17.27 – 17.27) m
Soil resistivity	100 Ω-m
Line length	100 km

For the given line, RLC matrices at 60 Hz are listed in (15).

$$R_{matrix}\left(\frac{\Omega}{km}\right)=\begin{bmatrix}0.11208 & 0.09848 & 0.09458\\ 0.09848 & 0.11504 & 0.09848\\ 0.09458 & 0.09848 & 0.11208\end{bmatrix}$$
$$L_{matrix}\left(\frac{H}{km}\right)=\begin{bmatrix}0.00139 & 0.00053 & 0.00041\\ 0.00053 & 0.00137 & 0.00053\\ 0.00041 & 0.00053 & 0.00139\end{bmatrix} \quad (15)$$
$$C_{matrix}\left(\frac{nF}{km}\right)=\begin{bmatrix}11.7781 & -1.71828 & -0.417076\\ -1.71828 & 12.0501 & -1.71826\\ -0.417076 & -1.71826 & 11.7781\end{bmatrix}$$

Positive-sequence and zero-sequence parameters at 60 Hz are listed in (16).

$$\begin{aligned}[R1,R0](\Omega/km) &= [0.01589 \quad 0.30742]\\ [L1,L0](H/km) &= [0.00090 \quad 0.00237]\\ [C1,C0](nF/km) &= [13.1533 \quad 9.29971]\end{aligned} \quad (16)$$

The two-source power system model used for real-time simulation to test the proposed line parameter estimation algorithm is shown in Fig. 17.

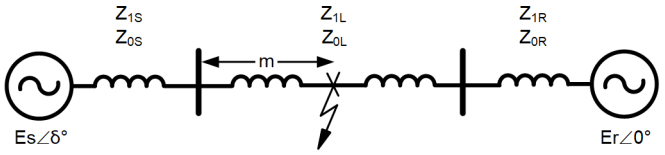

Fig. 17. Two-source power system model.

The transmission line Z1L and Z0L parameters are provided in Table I. The source impedances are shown in (17).

$$\begin{aligned}Z_{1S} &= 1.0 \bullet |Z_{1L}| \angle 82.3°\\ Z_{0S} &= 1.0 \bullet |Z_{0L}| \angle 66.9°\\ Z_{1R} &= 1.5 \bullet |Z_{1L}| \angle 82.3°\\ Z_{0R} &= 1.5 \bullet |Z_{0L}| \angle 66.9°\end{aligned} \quad (17)$$

XI. Acknowledgement

We would like to thank Greg Smelich of Schweitzer Engineering Laboratories, Inc. for providing the field events related to our research work and his support with this paper.

XII. References

[1] Power System Relay Committee, Working Group D6, "AC Transmission Line Model Parameter Validation," IEEE Power and Energy Society, September 2014.

[2] IEEE Std 1870-2019, *IEEE Guide for the Parameter Measurement of AC Transmission Lines*.

[3] IEEE Std 81-2012, *IEEE Guide for Measuring Earth Resistivity, Ground Impedance, and Earth Surface Potentials of a Grounding System.*

[4] H. Prado-Félix, V. Serna-Reyna, V. Mynam, M. Donolo, and A. Guzmán, "Improve Transmission Fault Location and Distance Protection Using Accurate Line Parameters," proceedings of GRIDTECH 2015, New Delhi, India, April 2015.

[5] A. Amberg, A. Rangel, and G. Smelich, "Validating Transmission Line Impedances Using Known Event Data," proceedings of the 65th Annual Conference for Protective Relay Engineers, College Station, TX, April 2012.

[6] D. Shi, D. J. Tylavsky, N. Logic, and K. M. Koellner, "Identification of Short Transmission-Line Parameters From Synchrophasor Measurements," proceedings of the 40th Annual North American Power Symposium, Calgary, Canada, September 2008.

[7] M. Grobler and R. Naidoo, "Determining Transmission Line Parameters From GPS Time-Stamped Data," proceedings of the 32nd Annual Conference on IEEE Industrial Electronics, Paris, France, November 2006.

[8] E. O. Schweitzer, A. Guzmán, V. Mynam, V. Skendzic, and B. Kasztenny, "Locating Faults by the Traveling Waves They Launch," proceedings of the 67th Annual Conference for Protective Relay Engineers, College Station, TX, April 2014.

[9] S. Marx, B. Johnson, A. Guzmán, V. Skendzic, and V. Mynam, "Traveling Wave Fault Location in Protective Relays: Design, Testing, and Results," proceedings of the 16th Annual Georgia Tech Fault and Disturbance Analysis Conference, Atlanta, GA, May 2013.

[10] D. Córton, J. Melado, J. Cruz, R. Kirby, Y. Korkmaz, G. Patti, and G. Smelich, "Double-Ended Traveling-Wave Fault Locating Without Relay-to-Relay Communications," proceedings of the 74th Annual Conference for Protective Relay Engineers, Virtual Format, March 2021.

[11] B. Kasztenny, A. Guzmán, N. Fischer, V. Mynam, and D. Taylor, "Practical Settings Considerations for Protective Relays That Use Incremental Quantities and Traveling Waves," proceedings of the 43rd Annual Western Protective Relay Conference, Spokane, WA, October 2016.

[12] E. O. Schweitzer, B. Kasztenny, A. Guzmán, V. Skendzic, and V. Mynam, "Speed of Line Protection – Can We Break Free of Phasor Limitations?" proceedings of the 68th Annual Conference for Protective Relay Engineers, College Station, TX, March 2015.

[13] G. Benmouyal and J. Roberts, "Superimposed Quantities: Their True Nature and Application in Relays," proceedings of the 30th Annual Western Protective Relay Conference, Spokane, WA, January 2003.

[14] B. Kasztenny, G. Benmouyal, H. J. Altuve, and N. Fischer, "Tutorial on Operating Characteristics of Microprocessor-Based Multiterminal Line Current Differential Relays," proceedings of the 38th Annual Western Protective Relay Conference, Spokane, WA, October 2011.

[15] J. Blackburn and T. Domin, *Protective Relaying: Principles and Applications (Third Edition)*, CRC Press, 2006.

[16] IEC 60255-121:2014, *Measuring Relays and Protection Equipment – Part 121: Functional Requirements for Distance Protection.*

XIII. Biographies

Arun Shrestha received his BSEE from the Institute of Engineering, Tribhuvan University, Nepal, in 2005, and his MS and PhD in electrical engineering from the University of North Carolina at Charlotte in 2009 and 2016, respectively. He joined Schweitzer Engineering Laboratories, Inc. (SEL) in 2011 as an associate power engineer in research and development. He is presently working as a senior engineer. His research areas of interest include power system protection and control design, real-time power system modeling and simulation, wide-area protection and control, power system stability, and digital substations. He is a senior member of IEEE and is a registered Professional Engineer. He is a member of IEEE PSRC and a U.S. representative to IEC 61850 TC 57 WG 10.

Sathish Kumar Mutha received his MS degree in electrical engineering in 2020 from the University of North Carolina at Charlotte. Prior to earning his MS degree, he worked as a power plant operation engineer in India. He joined Schweitzer Engineering Laboratories, Inc. (SEL) in 2019 as an engineer intern. He is currently a power engineer at SEL.